International Journal of Immunopathology & Pharmacology

Original Research Article

International Journal of Immunopathology and Pharmacology
2017, Vol. 30(3) 215–226

DOI: 10.1177/0394632017714696
journals.sagepub.com/home/iji
SAGE

Combinatorial antitumor effects of indoleamine 2,3-dioxygenase inhibitor NLG919 and paclitaxel in a murine B16-F10 melanoma model

Xiangjing Meng[1], Guangying Du[1], Liang Ye[2], Shanyue Sun[1], Qiaofeng Liu[1], Hongbo Wang[1], Wenyan Wang[1], Zimei Wu[1] and Jingwei Tian[1]

Abstract

Indoleamine 2,3-dioxygenase (IDO) is involved in tumor immune escape and resistance to chemotherapy, and is clinically correlated with tumor progression. IDO inhibitors show marginal efficacy as single agents; therefore, combinations of these inhibitors with other therapies hold promise for cancer therapy. The aim of this study was to investigate the synergistic antitumor effects of IDO inhibitor NLG919 in combination with different regimens of paclitaxel in a murine B16-F10 melanoma model. NLG919 increased the cytotoxic activity of paclitaxel toward B16-F10 cells in the presence of pretreatment with interferon (IFN)-γ in vitro. In B16-F10 tumor-bearing mice, NLG919 was uniformly distributed throughout tumors and decreased kynurenine levels and kynurenine/tryptophan ratios in tumors and plasma for 6–12 h. NLG919 suppressed tumor growth in a dose-dependent manner and exhibited maximum efficacy at 100 mg/kg. In combination with different regimens of paclitaxel, NLG919 displayed synergistic antitumor effects, and NLG919 did not increase the side effects of paclitaxel. Within the tumors, the percentage of $CD3^+$, $CD8^+$, and $CD4^+$ T cells and secretion of IFN-γ and interleukin-2 were synergistically increased, whereas the percentage of $CD4^+CD25^+$ regulatory T cells was decreased. NLG919 can potentiate the antitumor efficacy of paclitaxel without increasing its side effects, suggesting that the combination of IDO inhibitor-based immunotherapy with chemotherapy could be a potential strategy for cancer treatment.

Keywords

1-cyclohexyl-2-(5H-imidazo[5,1-a]isoindol-5-yl)ethanol (NLG919), chemotherapy, immunotherapy, indoleamine 2,3-dioxygenase, paclitaxel

Date received: 9 February 2017; accepted: 18 May 2017

[1]School of Pharmacy, Key Laboratory of Molecular Pharmacology and Drug Evaluation (Yantai University), Ministry of Education, Collaborative Innovation Center of Advanced Drug Delivery System and Biotech Drugs in Universities of Shandong, Yantai University, Yantai, P.R. China
[2]School of Public Health and Management, Institute of Toxicology, Binzhou Medical University, Yantai, P.R. China

Corresponding authors:
Guangying Du, School of Pharmacy, Key Laboratory of Molecular Pharmacology and Drug Evaluation (Yantai University), Ministry of Education, Collaborative Innovation Center of Advanced Drug Delivery System and Biotech Drugs in Universities of Shandong, Yantai University, Yantai 264005, P.R. China.
Email: guangyingdu@126.com

Jingwei Tian, School of Pharmacy, Key Laboratory of Molecular Pharmacology and Drug Evaluation (Yantai University), Ministry of Education, Collaborative Innovation Center of Advanced Drug Delivery System and Biotech Drugs in Universities of Shandong, Yantai University, Yantai 264005, P.R. China.
Email: tianjeanswest@gmail.com

Introduction

Immune checkpoint therapies target regulatory pathways that affect T cells to enhance antitumor immune responses and have been used for clinical treatment of cancer following the approval of ipilimumab, pembrolizumab, nivolumab, and atezolizumab by the Food and Drug Administration (FDA).[1,2] Indoleamine 2,3-dioxygenase (IDO), an investigational immune checkpoint target, catalyzes the initial and rate-limiting steps in the metabolism of the essential amino acid tryptophan (Trp) along the L-kynurenine (Kyn) pathway.[3] Recent studies suggest that IDO is involved in tumor-induced escape from immune surveillance through the local depletion of Trp and accumulation of its toxic metabolite.[4,5] IDO is overexpressed in various human cancers such as melanoma, ovarian cancer, and colorectal cancer, and its expression level is clinically correlated with tumor progression and poor clinical outcomes.[6] Thus, IDO may be a therapeutic target for malignant cancer. Four IDO inhibitors have been entered in clinical trials: epacadostat (Incyte, phase 3), indoximod (NewLink, phase 2), BMS-986205 (Bristol-Myers Squibb, phase 1), and GDC-0919 (Genentech, phase 1).[7]

IDO inhibitors are only marginally efficacious as single agents in preclinical studies.[8,9] Therefore, the combination of IDO inhibitor with chemotherapy or other immune checkpoint therapy holds promise for cancer therapy.[10,11] There is evidence indicating that IDO inhibitors can enhance the efficacy of common chemotherapeutics which included paclitaxel (PTX), cisplatin, doxorubicin, and temozolomide.[8,12] Although PTX is characterized as a mitotic inhibitor, it also displays immunestimulatory effects against tumors by promoting T-cell infiltration and activation.[13]

NLG919, an imidazoleisoindole derivative with its chemical structure shown in Figure 1, was developed by NewLink and later licensed to Genentech as GDC-0919 or RG-6078, which is undergoing a phase 1 clinical trial.[14] Only a few efficacy reports of NLG919 were obtained at AACR meetings in the form of abstracts.[14] The details of antitumor activity of NLG919 or its combination with PTX have not yet been reported. Therefore, the main aim of this study was to investigate the synergistic antitumor functions of NLG919 and PTX in a murine B16-F10 melanoma model.

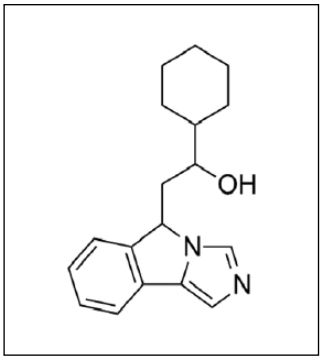

Figure 1. Chemical structure of NLG919.

Methods

Chemicals and reagents

NLG919 (CAS: 1402836-58-1), with batch number 2015073101 and purity >98.5%, was obtained from Hanxiang Biological Technology Co., Ltd. (Shanghai, China). The chemical name of NLG919 is 1-cyclohexyl-2-(5H-imidazo[5,1-a] isoindol-5-yl)ethanol, with the molecular formula $C_{18}H_{22}N_{20}$ and molecular weight of 282.4. For in vitro experiments, NLG919 was dissolved in dimethyl sulfoxide (DMSO) and diluted with Dulbecco's modified Eagle's medium (DMEM) to the desired concentration. For in vivo experiments, NLG919 was reconstituted in aqueous 1% sodium carboxymethyl cellulose SCMC (w/v) to the desired concentration. PTX (TAXOL®), 30 mg/5 mL per vial, manufactured by Bristol-Myers Squibb, was diluted to the appropriate concentrations with 0.9% sodium chloride. Fluorescein-5-isothiocyanate (FITC)-conjugated rat anti-mouse CD3 (Catalog No. 555274), FITC-conjugated rat anti-mouse CD4 (Catalog No. 553729), phycoerythrin (PE)-conjugated rat anti-mouse CD8a (Catalog No. 553033), and allophycocyanin (APC)-conjugated rat anti-mouse CD25 (Catalog No. 558643) antibodies were purchased from BD Biosciences. Mouse interleukin (IL)-2 quantitative enzyme-linked immunosorbent assay (ELISA) kit (Catalog No. M2000) and mouse interferon (IFN)-γ quantitative ELISA kit (Catalog No. MIF00) were purchased from R&D Systems. Collagenase A, hyaluronidase (type V), and DNase I were purchased from Sigma–Aldrich. Fetal bovine serum (FBS) and DMEM (Gibco™) were obtained from Life Technologies Corporation.

Cell culture and animals

The murine melanoma cell line B16-F10 was kindly provided by Cell Bank, Chinese Academy of Sciences. The cells were cultured in DMEM supplemented with 10% FBS, 2 mM L-glutamine, 50 IU/mL penicillin, and 50 μg/mL streptomycin sulfate and maintained at 37°C in a humidified atmosphere containing 5% CO_2.

Five- to six-week-old male C57BL/6 mice were purchased from Beijing Vital River Laboratory Animal Technology Co., Ltd. The animal production license number was SCXK (Jing) 2012-0001. The animals were quarantined and equilibrated to the new environment for 7 days and maintained in a specific pathogen-free (SPF) environment with free access to sterilized food and water. The animal room was maintained on a 12-h light/dark cycle at 21°C ± 5°C and 55% ± 15% relative humidity.

B16-F10 tumor-bearing mouse model

On day 0 of the experiment, the animals were subcutaneously inoculated in the dorsal scapular with 0.2 mL of Matrigel (BD Pharmingen) containing 1×10^5 tumor cells (1:1 volume Matrigel/tumor cells) under ketamine-xylazine anesthesia. The width (W) and length (L) of the B16-F10 xenografts were measured by calipers, and the tumor volume (V) was calculated according to the following formula: $V = 0.5 \times L \times W^2$. All animal experiments were performed in accordance with the animal experimentation guide and protocols approved by the Experimental Animal Research Committee of Yantai University.

Sensitivity of B16-F10 cells to PTX induced by NLG919 in vitro

Given that IDO is also positively associated with resistance to PTX-based chemotherapy,[15] we asked whether NLG919 can enhance the sensitivity of tumors to PTX. B16-F10 cells were diluted to 1×10^5 cells/mL with DMEM supplemented with 10% FBS and seeded at 2 mL per well into 6-well plates. The culture medium was replaced with fresh growth medium with or without 25 ng/mL IFN-γ for 10–12 h after seeding. After incubation with IFN-γ for 24 h, the medium was replaced with fresh medium containing 100 nM NLG919, 3 nM PTX, or a combination of 100 nM NLG919 and 3 nM PTX, and medium containing 0.1% DMSO was used as the vehicle treatment. PTX at 3 nM was a concentration with low inhibition rate (IR) of cell growth about 20%. At 0, 12, 24, 48, and 72 h after addition of drugs, cells were washed to remove dead cells and particles. Adherent cells were trypsinized and counted using a CountStar IC1000 Automated Cell Counter (Ruiyu-Biotech). Viability of the counted cells was confirmed by 0.1% trypan blue exclusion. The effect of NLG919 and PTX on the growth of cells was analyzed by plotting cell growth curves using viable cell numbers against time.

Determination of Trp and Kyn levels in the B16-F10-bearing mice

To further verify the biochemical mechanism of NLG919, the levels of Kyn and Trp in the plasma, tumors, and tumor-draining lymph nodes (TDLNs) were observed for a single dose of NLG919. The methods for quantification of Trp and Kyn combined a protein-precipitation extraction using trichloroacetic acid and liquid chromatography tandem-mass spectrometry (LC-MS/MS) analysis. The method for quantification of NLG919 combined a protein-precipitation extraction using acetonitrile and LC-MS/MS analysis.

When the B16-F10 tumor xenografts reached approximately 300–400 mm^3 in volume, the mice were given a single dose of 100 mg/kg NLG919 via intragastric (i.g.) administration. At 0, 1, 2, 6, 12, and 24 h after administration, samples of plasma, tumor, and TDLN were collected for detection of NLG919, Trp, and Kyn in five animals per time point. The plasma samples were diluted 10-fold in water. Tumors and lymph nodes were homogenized in 5% acetonitrile in water with 0.1% formic acid and diluted depending on the weight-to-volume ratio—3 for tumors and 10 for lymph nodes. The homogenates were centrifuged, and supernatants were collected for sample analysis. The Kyn/Trp ratio was calculated after Kyn and Trp levels were determined.

Dose-dependent antitumor effects of NLG919

One day after the B16-F10 tumor cells were inoculated into mice, the tumor-bearing mice were randomized into four groups: vehicle group and 50, 100, and 200 mg/kg NLG919 groups. Each group contained 12 animals. The animals in the vehicle and NLG919 groups were dosed with SCMC and NLG919, respectively, twice daily from day 1 to

day 16 via i.g. administration. The tumor volumes were measured once every 2 days from day 6 to day 16, and animal body weights were measured once every 2 days during the whole study. Two hours after the last dose on day 16, the tumors were dissected out and weighed, and the mean tumor weight (MTW) in each group was obtained. The IR% of tumor weights was calculated by the following formula: $IR(\%) = [(MTW_{\text{vehicle group}} - MTW_{\text{treatment group}})/MTW_{\text{vehicle group}}] \times 100$.

After quickly weighing, six tumors were randomly selected from each group and used to determine the level of Kyn as described in section "Determination of Trp and Kyn levels in the B16-F10-bearing mice."

Combinatorial treatment with NLG919 and PTX

To study the combined antitumor effects of NLG919 and PTX, single doses of NLG919 and three different regimens of PTX were used in this study. The dose of NLG919 in each corresponding group was 100 mg/kg via i.g. administration twice a day. The three PTX regimens were as follows: (1) PTX13(2/w): 13 mg/kg, twice a week; (2) PTX13(1/w): 13 mg/kg, once a week; and (3) PTX6.5(2/w): 6.5 mg/kg, twice a week; all administered by intravenous (i.v.) injection. On day 1 of the experiment, the B16-F10 tumor-bearing mice were randomized into eight groups: vehicle group (SCMC, i.g., twice a day), NLG919 group, PTX13(2/w) group, NLG919 + PTX13(2/w) group, PTX13(1/w) group, NLG919 + PTX13(1/w) group, PTX6.5(2/w) group, and NLG919 + PTX6.5(2/w) group. Each group contained 12 animals. SCMC, PTX, and NLG919 were administered according to the above doses, routes, and frequencies from day 1 to day 17, with the dosing volume measured in mL/10 g. The tumor volumes were measured once every 2 days from day 7 to day 17, and animal body weights were measured once every 2 days during the whole study. At the end of the study, the tumors were dissected out and weighed, and the IR of tumor weight was calculated.

Immunological mechanisms of the antitumor effects of NLG919 in combination with PTX

The grouping, dose, and route of administration were the same as described in section "Combinatorial treatment with NLG919 and PTX." Each group contained 10 animals. The animals were treated with PTX and/or NLG919 from day 1 to day 9. At the end of treatment, the T-cell populations and cytokines within tumors were analyzed.

Preparation of tumor-infiltrating lymphocytes. Tumor-infiltrating lymphocytes (TILs) were harvested from the tumors. Single-cell suspensions were prepared according to a previously described protocol with a few modifications.[16] The mice were euthanized and disinfected with 75% alcohol for 2 min; then, the tumors were dissected out and weighed. Using sterile scissors and forceps, the tumors were dissociated into small pieces and immersed in digestion buffer (5 mL per 0.25 g of tumor tissue). The digestion buffer was composed of DMEM containing 5% FBS, 0.5 mg/mL collagenase A, 0.2 mg/mL hyaluronidase, and 0.02 mg/mL DNase I. The mixture was incubated at 37°C for 30 min, and the resulting cell suspensions were filtered through a 200-mesh sieve. After centrifugation at 1500 g for 5 min, the cells were washed and adjusted to a density of 10^7 cells/mL. This suspension was separated using a separating medium kit for mouse TILs (LTS1092Z; TBD Science) and centrifuged for 20 min at 2000 g. Cells at the interface (TIL) were carefully harvested and transferred to a sterile tube, and then washed twice with cold DMEM containing 2% FBS.

Flow cytometry. Three-color staining of lymphocytes was performed with FITC-conjugated anti-mouse CD3 and CD4 antibodies, PE-conjugated anti-mouse CD8 antibody, and APC-conjugated anti-mouse CD25 antibody. TILs from two mice were combined and subsequently stained with antibodies to the various T-cell markers using standard staining methods. Fluorescence-activated cell sorting (FACS) was conducted with an Accuri™ C6 flow cytometer, and the data were analyzed with CFlow Plus software (BD Biosciences).

Determination of IFN-γ and IL-2 levels by ELISA. TILs were normalized for CD3-positive cells by flow cytometry and cultured in DMEM containing 5% FBS, 1 mM HEPES, 25 μM 2-mercaptoethanol, 50 IU/mL penicillin, and 50 μg/mL streptomycin sulfate. TILs were adjusted to 1×10^5 cells/mL with DMEM supplemented with 5% FBS, and 2 mL of cells were seeded per well in 24-well plates. After the

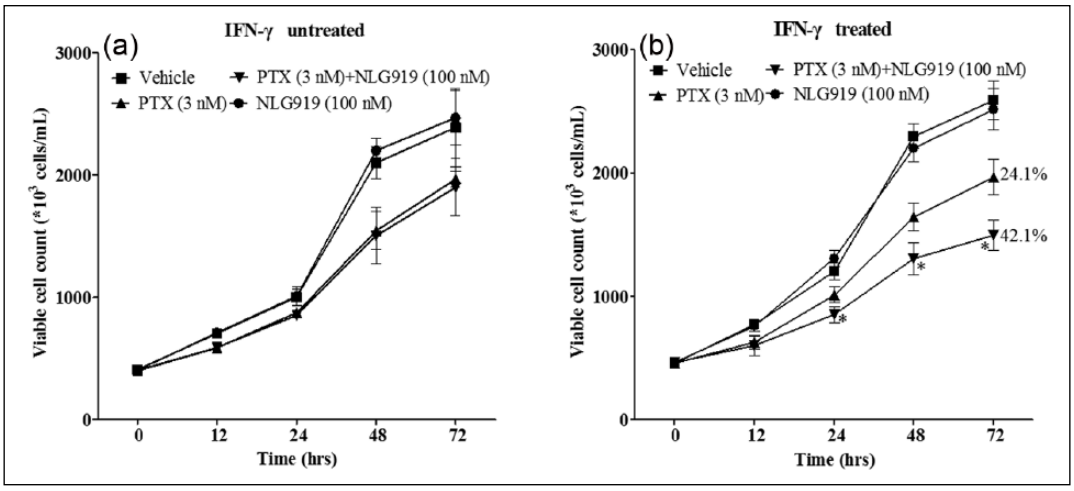

Figure 2. NLG919 increased the sensitivity of B16-F10 cells to paclitaxel after treatment with IFN-γ. B16-F10 cells were cultured with or without 25 ng/mL IFN-γ for 24 h, and the medium was then replaced with fresh growth medium containing 3 nM paclitaxel (PTX), 50 nM NLG919, or a combination of both, and medium containing 0.1% dimethyl sulfoxide was used as the vehicle. The cells were cultured for 0, 12, 24, 48, and 72 h, cell viability was measured, and cell growth curves were drawn. (a) Cells were not pre-treated with IFN-γ; (b) cells were pre-treated with IFN-γ. *$P < 0.05$ compared with the PTX group; the inhibition rates of cell proliferation in the PTX plus NLG919 group and the PTX group at 72 h were 42.1% and 24.1%, respectively.

cells were cultured for 24 h without stimulation, the supernatants were harvested for the determination of IFN-γ and IL-2 levels using the mouse IFN-γ ELISA kit and IL-2 ELISA kit, respectively.

Statistical analysis

The results are presented as the mean ± SD, and $P < 0.05$ was considered statistically significant. The data were analyzed by two-tailed unpaired Student's t-tests for paired groups or one-way analysis of variance (ANOVA) for three or more groups with the PASW Statistics 18.0 software package.

Results

NLG919 sensitizes B16-F10 cells to PTX in vitro

It has been reported that IDO is involved in the regulation of tumor resistance to PTX.[15] Therefore, the effects of NLG919 on the sensitivity of B16-F10 cells to PTX were preliminarily studied in this study. B16-F10 cells were treated with or without IFN-γ for 24 h and then with 3 nM PTX, 50 nM NLG919, or a combination 3 nM PTX with 50 nM NLG919 for 0–72 h. As shown in Figure 2, no obvious effects on cell proliferation were observed at any time point in the NLG919-treated cells regardless of IFN-γ induction. The effect of PTX alone on the suppression of cell proliferation was small, with an IR of approximately 20%, regardless of IFN-γ induction. Before IFN-γ induction, there were no significant differences in cell numbers between the PTX plus NLG919 group and the PTX group (Figure 2(a)). However, after IFN-γ induction, the cell number in the PTX plus NLG919 group was significantly lower than that in the PTX group after 24 h ($P < 0.05$), and the IRs of cell proliferation were 42.1% and 24.1% at 72 h, respectively (Figure 2(b)). These data showed that NLG919 could significantly increase the sensitivity of B16-F10 cells to PTX in vitro.

Determination of Trp and Kyn levels in the B16-F10-bearing mice treated with NLG919

To investigate and confirm the biochemical mechanism of NLG919, the levels of Kyn, Trp, and NLG919 were determined in the plasma, tumors, and TDLN after the B16-F10 tumor-bearing mice were given a single dose of NLG919 at 100 mg/kg via i.g. administration. As shown in Figure 3(a), NLG919 was distributed to a greater extent in the tumors than in the plasma and TDLN, and the high concentrations in the different tissues were maintained for approximately 3–4 h post dosing. No obvious changes in the levels of Trp were noted in the three tissues (Figure 3(b)). The levels of Kyn in the tumor and plasma samples were significantly decreased from 1 to 12 h and from 1 to 6 h after

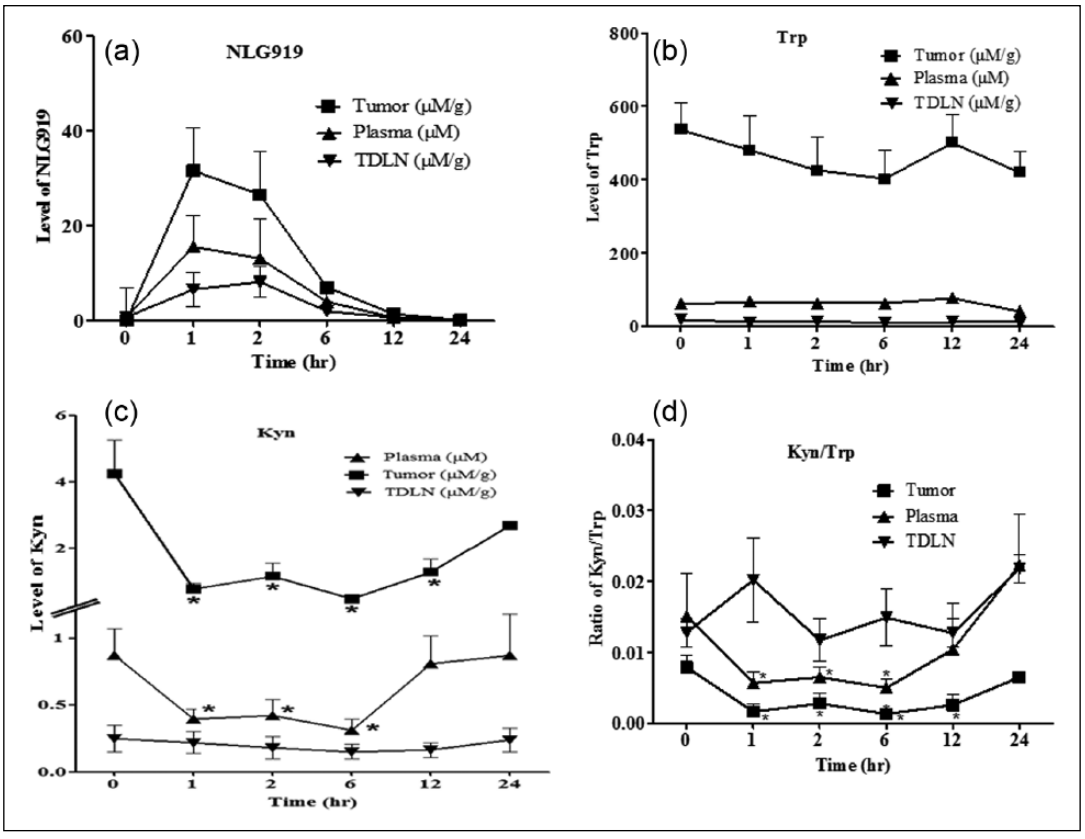

Figure 3. Levels of Trp and Kyn in the plasma, tumor, and TDLN. B16-F10 tumor-bearing mice were intragastrically administered with a single dose of NLG919 at 100 mg/kg. At 0, 1, 2, 6, 12, and 24 h after dosing, samples of plasma, tumors, and TDLN were collected for the detection of NLG919, Trp and Kyn (n = 5). All samples were analyzed via liquid chromatography tandem-mass spectrometry. The Kyn/Trp ratio was calculated after the levels of Kyn and Trp were determined. (a–d) Levels of NLG919, Trp, Kyn, and Kyn/Trp, respectively. *$P < 0.05$ compared with the value at 0 h.

drug administration, respectively ($P < 0.05$), while no obvious change was observed in TDLN (Figure 3(c)). Similar to the changes in Kyn, the ratios of Kyn/Trp in the tumor and plasma sample were significantly reduced from 1 to 12 h and from 1 to 6 h, respectively ($P < 0.05$), while no obvious change was observed in TDLN (Figure 3(d))

Dose-dependent antitumor efficacy of NLG919

To evaluate the dose-dependent antitumor effects of NLG919, B16-F10 tumor-bearing mice were intragastrically administered with NLG919 twice daily at different doses for 16 consecutive days. As shown in Figure 4(a), growth suppression was observed in the tumors in response to NLG919 at 50, 100, and 200 mg/kg in a dose-dependent manner. The inhibitory effects of NLG919 at 100 and 200 mg/kg on tumor growth were better than that at 50 mg/kg, while there was no significant difference between the doses of 100 and 200 mg/kg. At the end of the study, the MTWs in the 50, 100, and 200 mg/kg NLG919 groups were markedly lower than those in the vehicle group ($P < 0.05$), and the tumor IRs were 25.6%, 46.0%, and 45.4% (Figure 4(b)), respectively. Compared with NLG919 at 50 mg/kg, NLG919 at 100 and 200 mg/kg exhibited stronger effects on tumor regression ($P < 0.05$), while no significant difference in the MTW was observed between the 100 and 200 mg/kg groups ($P > 0.05$). No significant effects on the body weight of tumor-bearing mice were observed in any of the NLG919 groups (data not shown).

To understand the changes in the biomarker Kyn, the levels of Kyn in six randomly selected tumors from each group were determined. As shown in Figure 4(c), compared with the vehicle group, a significant decrease in Kyn levels was observed in the 50, 100, and 200 mg/kg NLG919 treatment groups ($P < 0.05$), with Kyn IRs of 66.1%, 83.5%, and 84.5%, respectively. The levels of Kyn with NLG919 at 100 and 200 mg/kg

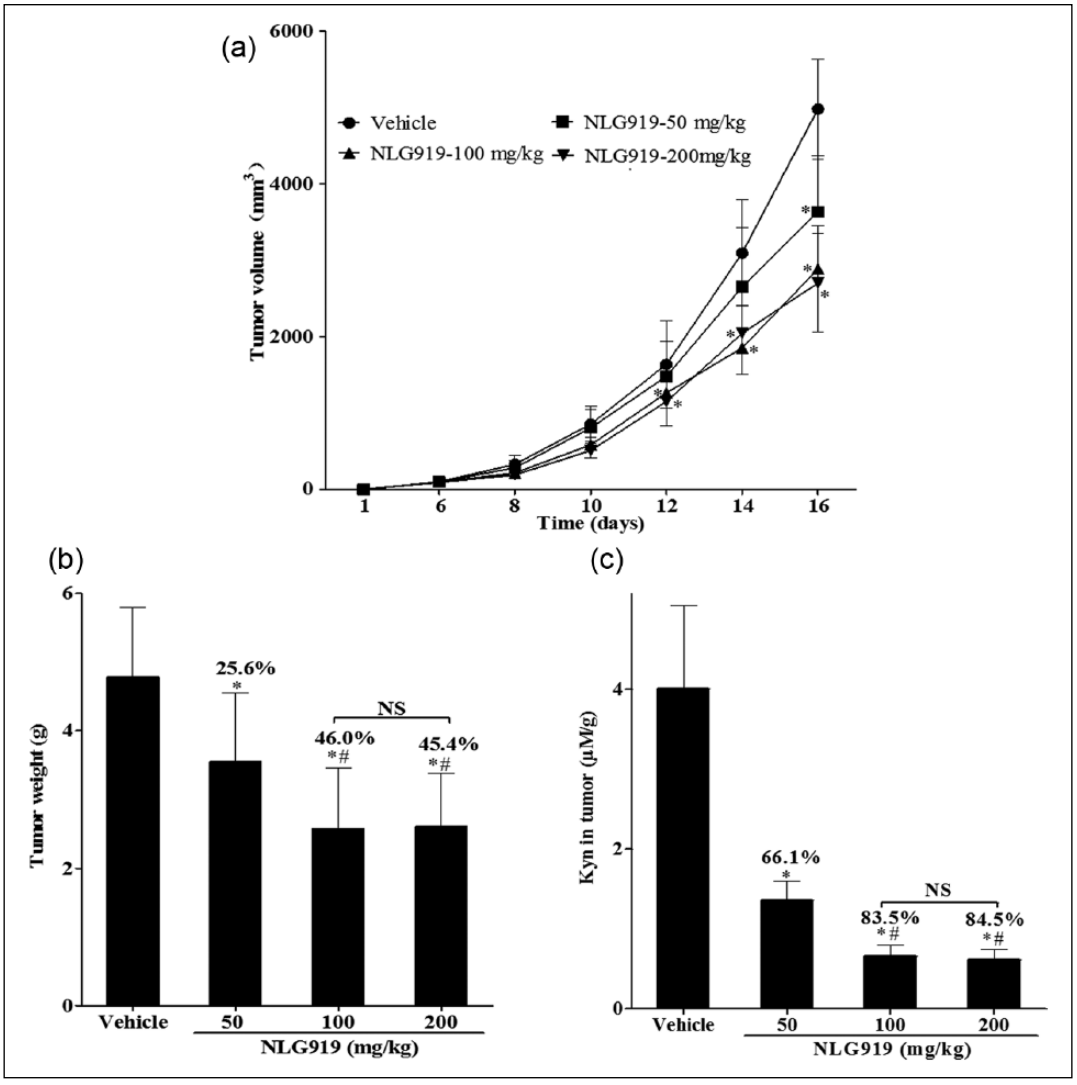

Figure 4. Dose-dependent antitumor efficacy of NLG919. B16-F10 tumor-bearing mice were randomized into vehicle group, NLG919 50, 100, and 200 mg/kg groups (n = 12). The animals were intragastrically administered with 1% sodium carboxymethyl cellulose (SCMC) or NLG919 twice daily from day 1 to day 16. The tumors were dissected out and weighed 2 h after the last dose, and the levels of Kyn in the tumors were determined by liquid chromatography tandem-mass spectrometry (n = 6). The inhibition rate of tumor weight and Kyn levels were determined. (a) Tumor growth curve; (b) mean tumor weight and inhibition rate; (c) level of Kyn in the tumors and the inhibition rate. *$P < 0.05$ compared with the vehicle group; #$P < 0.05$ compared with the NLG919 50 mg/kg group; NS: not significant.

were also significantly lower than those with NLG919 at 50 mg/kg, while no significant difference was observed between 100 and 200 mg/kg ($P > 0.05$).

Combinatorial treatment with NLG919 and PTX

The data from the dose-dependence study showed that NLG919 at 100 mg/kg demonstrated the maximum antitumor efficacy. Therefore, 100 mg/kg was used in the subsequent experiments. The animals bearing B16-F10 tumors were intragastrically administered with SCMC or 100 mg/kg NLG919 twice daily from day 1 to day 17 or intravenously administered with different regimens of PTX, or treated with combinations of NLG919 and PTX. Different doses (13 or 6.5 mg/kg) and different frequencies (twice a week or once a week) of PTX were used in this study, which corresponded to the three PTX regimens: PTX13(2/w), PTX13(1/w), and PTX6.5(2/w).

As shown in Figure 5(a), suppression of tumor volume was observed in the NLG919-only,

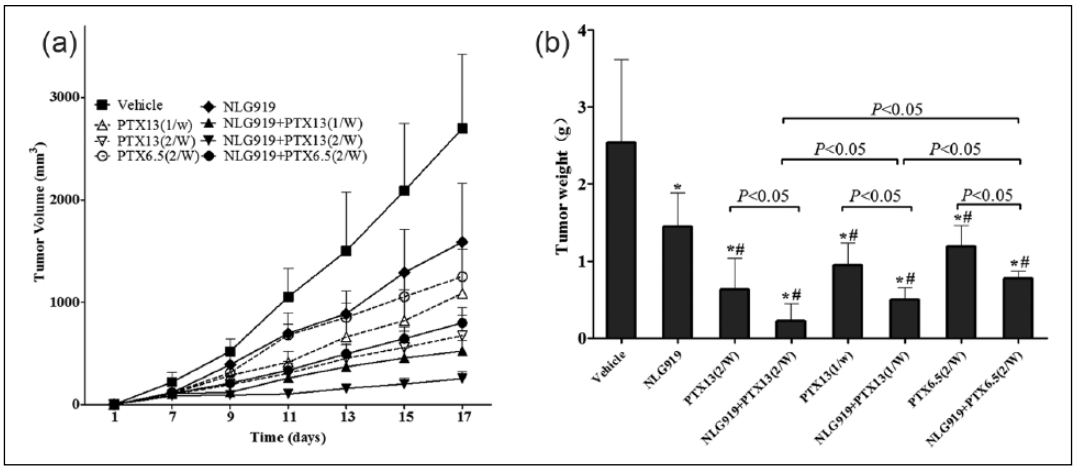

Figure 5. Combinatorial treatment with NLG919 and paclitaxel. Animals bearing B16-F10 tumors (n = 12) were intragastrically administered with 1% SCMC or 100 mg/kg NLG919 twice daily, intravenously administered with PTX, or treated with combinations of NLG919 and PTX from day 1 to day 17. Three PTX regimens were used as follows: (1) PTX13(2/w): 13 mg/kg, twice a week; (2) PTX13(1/w): 13 mg/kg, once a week; and (3) PTX6.5(2/w): 6.5 mg/kg, twice a week. Tumor growth and body weight were monitored during the study. Tumor weights were measured on day 17, and the inhibition rate was calculated. (a) Tumor growth curve; (b) mean tumor weight. $^{*}P < 0.05$ compared with the vehicle group; $^{\#}P < 0.05$ compared with the NLG919 100 mg/kg group.

Table 1. Effects of the combination of NLG919 and paclitaxel (PTX) on body weight and B16-F10 xenograft tumor weights.

Groups	Body weight (g)			Tumor weight (g)	Inhibition rate (%)
	Pre-treatment (day 1)	Post-treatment (day 17)	Weight gain (%)		
Vehicle	21.5 ± 1.8	22.9 ± 2.2$^{\&}$	6.5	2.54 ± 1.08	–
NLG919	21.9 ± 1.5	22.3 ± 2.4	1.8	1.45 ± 0.44*	42.9
PTX13(2/W)	21.8 ± 1.2	19.5 ± 2.7$^{\&}$	−10.6	0.63 ± 0.31$^{*,\#}$	75.3
NLG919+PTX13(2/W)	21.7 ± 1.3	19.8 ± 1.8$^{\&}$	−8.8	0.22 ± 0.15$^{*,\#,a}$	91.2
PTX13(1/w)	22.0 ± 1.5	20.7 ± 2.0$^{\&}$	−5.9	0.95 ± 0.28$^{*,\#}$	62.6
NLG919+PTX13(1/W)	21.3 ± 1.7	20.4 ± 1.3	−4.2	0.49 ± 0.16$^{*,\#,b,d}$	80.5
PTX6.5(2/W)	21.8 ± 1.1	21.3 ± 1.7	−2.3	1.18 ± 0.28$^{*,\#}$	53.3
NLG919+PTX6.5(2/W)	21.6 ± 1.2	21.2 ± 1.9	−1.9	0.77 ± 0.21$^{*,\#,c,d,e}$	69.7

Animals bearing B16-F10 tumors (n = 12) were intragastrically administered with 1% SCMC or 100 mg/kg NLG919 twice daily, intravenously administered with PTX, or treated with combinations of NLG919 and PTX from day 1 to day 17. Three PTX regimens were used as follows: (1) PTX13(2/w): 13 mg/kg, twice a week; (2) PTX13(1/w): 13 mg/kg, once a week; and (3) PTX6.5(2/w): 6.5 mg/kg, twice a week. The percentage of body weight gain was calculated based on the values at the beginning of the study. Tumor weight was measured on day 17, and the IR was calculated. The data are presented as the means ± SD.

$^{\&}P < 0.05$ compared with body weight at beginning of the study.

$^{*}P < 0.05$ compared with the vehicle group.

$^{\#}P < 0.05$ compared with the NLG919 group.

$^{a,b,c}P < 0.05$ compared with the PTX13(2/W), PTX13(1/W), and PTX6.5(2/W) groups, respectively.

$^{d,e}P < 0.05$ compared with the NLG919+PTX13(2/W) and NLG919+PTX13(1/W) groups, respectively.

PTX-only (all three dosages), and combinatorial treatment groups. NLG919 combined with PTX in different regimens exhibited synergistic antitumor effects. As shown in Figure 5(b) and Table 1, the MTWs in the NLG919, PTX, and combinatorial treatment groups were all significantly lower than that in the vehicle group ($P < 0.05$). The MTWs in the PTX and combinatorial treatment groups were significantly lower than those in the NLG919 group ($P < 0.05$). The MTWs in NLG919+PTX13(2/w), NLG919+PTX13(1/w), and NLG919+PTX6.5(2/w) groups were all significantly lower than those in the NLG919-only group and the corresponding PTX group ($P < 0.05$), exhibiting 15.9%, 17.9%, and 16.4% increase in the IR, respectively, when compared to the corresponding PTX-only groups. For the three combinatorial treatment groups, the MTW in the NLG919+PTX13(1/w) group was significantly lower than that in the NLG919+PTX13(2/w)

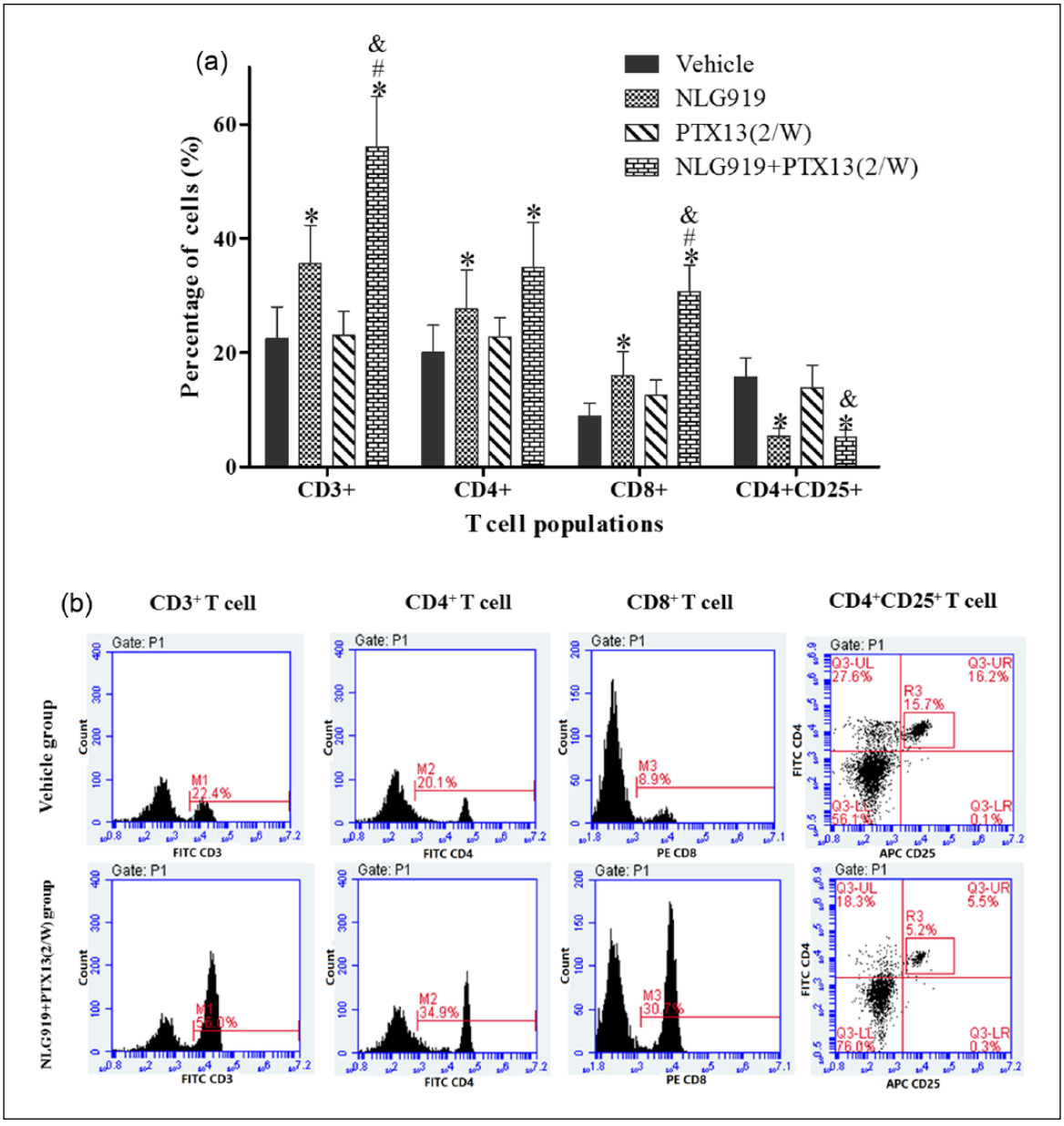

Figure 6. T-cell populations in the B16-F10 tumors. Animals bearing B16-F10 tumors (n = 10) were intragastrically administered with 1% SCMC or 100 mg/kg NLG919 twice daily, intravenously administered with 13 mg/kg PTX twice a week, or treated with a combination of NLG919 and PTX, from day 1 to day 9. On day 9, tumor-infiltrating lymphocytes were combined for every two mice and analyzed by flow cytometry with FITC-conjugated anti-mouse CD3 and CD4 antibodies, PE-conjugated anti-mouse CD8 antibody, and APC-conjugated anti-mouse CD25 antibody. (a) Representative T-cell populations from the NLG919+PTX13(2/W) group; (b) representative flow graphs. The frequencies of $CD4^+$ and $CD8^+$ cells were represented as the percentage of $CD3^+$ cells. *$P < 0.05$ compared with the vehicle group; #$P < 0.05$ compared with the NLG919 100 mg/kg group; &$P < 0.05$ compared with the PTX group.

group and significantly higher than that in the NLG919+PTX6.5(2/w) group, with IRs of 80.5%, 91.2%, and 69.7%, respectively.

No significant effect on the body weight of tumor-bearing mice was observed in the NLG919 group. A dose-dependent decrease in the body weight was noted in the PTX groups (Table 1), and the body weight decreased by 10.6% in the PTX13(2/w) group compared to that at the beginning of the study ($P < 0.05$). No decrease in body weight was observed in the combinatorial treatment groups when compared with the corresponding PTX groups, that is, NLG919 did not increase the side effects of PTX.

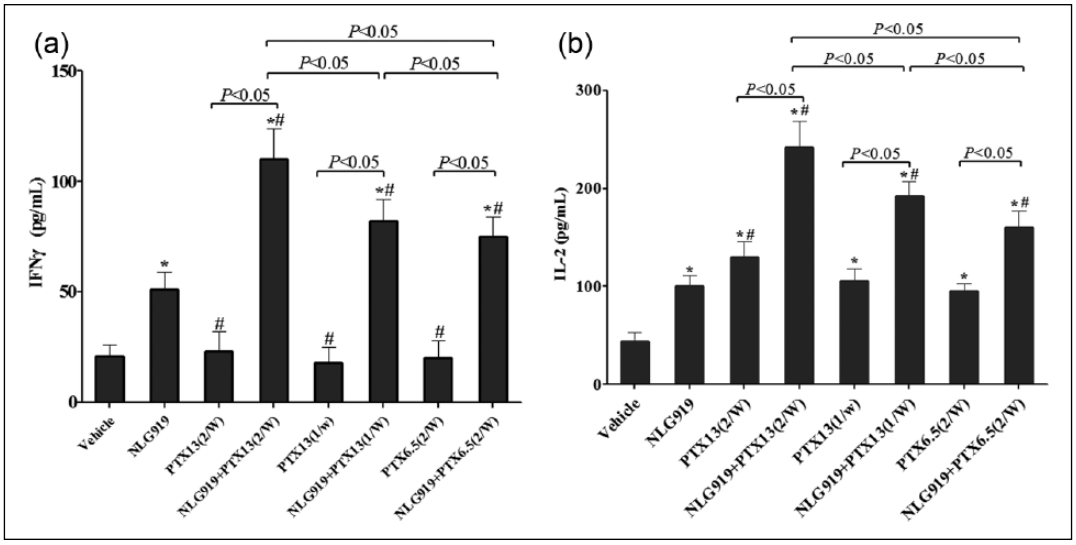

Figure 7. Determination of concentration of (a) IFN-γ and (b) IL-2 secreted by tumor-infiltrating lymphocytes (TILs). Animals bearing B16-F10 tumors (n = 10) were intragastrically administered with 1% SCMC or 100 mg/kg NLG919 twice daily, intravenously administered with different regimens of PTX, or treated with combinations of NLG919 and PTX, from day 1 to day 9. Three PTX regimens were used as follows: (1) PTX13(2/w): 13 mg/kg, twice a week; (2) PTX13(1/w): 13 mg/kg, once a week; and (3) PTX6.5(2/w): 6.5 mg/kg, twice a week. On day 9, TILs were harvested from the tumors. Tumor-infiltrating lymphocytes were pooled for every two mice and seeded into 24-well plates at 2×10^5 cells/well and in triplicate wells for each group. After the cells were cultured for 24 h, the supernatants were harvested for the determination of IFN-γ and IL-2 concentrations by ELISA. *$P < 0.05$ compared with the vehicle group; #$P < 0.05$ compared with the NLG919 100 mg/kg group.

Immunological mechanisms of the antitumor effects of NLG919 and PTX

To understand the immunological mechanisms of antitumor effects of the combinatorial treatment with NLG919 and PTX, T-cell populations ($CD3^+$, $CD4^+$, $CD8^+$, and $CD4^+CD25^+$) and cytokines (IFN-γ and IL-2) within tumors were analyzed after the B16-F10 tumor-bearing mice were treated with SCMC, PTX, or NLG919 for 9 days.

T-cell population analysis. The representative results of the analysis of the NLG919+PTX13(2/w) group and single-treatment groups by flow cytometry are shown in Figure 6. An increase in the percentage of $CD3^+$, $CD8^+$, and $CD4^+$ T cells and a decrease in the percentage of $CD4^+CD25^+$ Tregs were noted in the NLG919 group. Thus, there was a shift in the ratio of effector to regulatory T cells (Teff/Treg) from 0.57 to 2.94. Only a slight increase in the percentage of $CD3^+$, $CD8^+$, and $CD4^+$ T cells and a slight decrease in the percentage of $CD4^+CD25^+$ Tregs were noted in the PTX groups.

Compared with the vehicle group, a significant increase in the percentage of $CD3^+$, $CD8^+$, and $CD4^+$ T cells and a decrease in the percentage of $CD4^+CD25^+$ Tregs were noted in the combined treatment groups. When compared with the NLG919 group, the percentage of $CD4^+$ T cells and $CD4^+CD25^+$ Tregs in the combined treatment group was not notably changed; however, significant changes in the number of $CD8^+$ T cell were found, indicating that the increase in $CD8^+$ T cells might be one of the reasons by which PTX enhances the antitumor activity of NLG919. The Teff/Treg ratio in the combined treatment group was 5.90, which was clearly higher than that in the vehicle (0.57), NLG919 (2.94), and PTX (0.89) groups. Among the three combined treatment groups, the number of $CD8^+$ T cell and Teff/Treg in the NLG919+PTX13(2/W) group was higher than those in the other two groups.

Cytokine analysis. The function of lymphocytes infiltrating the B16-F10 tumors was determined by measuring the concentration of secreted IFN-γ and IL-2. TILs were harvested from the tumors after 9 days of NLG919, PTX, or combined treatment. After the TILs were cultured for 24 h, IFN-γ and IL-2 levels in the supernatants were determined by ELISA.

The results of IFN-γ detection are shown in Figure 7(a). The activity of TILs was enhanced by

NLG919, with a 2.43-fold increase in the release of IFN-γ ($P<0.05$). The concentration of IFN-γ in the three PTX groups exhibited no significant difference compared to that in the vehicle group and was significantly lower than that in the NLG919 group ($P<0.05$). The concentration of IFN-γ in all the combinatorial treatment groups was significantly higher than that in the vehicle group ranging from 3.68- to 5.21-fold and was significantly higher than that in the NLG919 group or PTX group ($P<0.05$). For the combinatorial treatment groups, the concentration of IFN-γ in the NLG919+PTX13(1/w) group was significantly higher than that in the NLG919+PTX6.5(2/w) group and significantly lower than that in the NLG919+PTX13(2/w) group ($P<0.05$).

The results of IL-2 detection are shown in Figure 7(b). A significant increase in the concentration of IL-2 was noted in the NLG919 group, which was 2.27-fold higher than that in the vehicle group ($P<0.05$). The concentration of IL-2 in all the PTX groups was significantly higher than that in the vehicle group ranging from 2.16- to 2.95-fold ($P<0.05$). The concentration of IL-2 in the PTX13(2/w) group was significantly higher than that in the NLG919 group ($P<0.05$). The concentration of IL-2 in all the combinatorial treatment groups was significantly higher than that in the vehicle group ranging from 3.55- to 5.57-fold and was significantly higher than that in the NLG919 group or PTX single-agent group ($P<0.05$). For the combinatorial treatment groups, the concentration of IL-2 in the NLG919+PTX13(1/w) group was significantly higher than that in the NLG919+PTX6.5(2/w) groups and significantly lower than that in the NLG919+PTX13(2/w) group ($P<0.05$).

Discussion

IDO is a key immunosuppressive enzyme that modulates antitumor immune responses by promoting regulatory T-cell production and blocking effector T-cell activation. Targeting IDO may be a promising approach that could reverse the complex processes in tumor immune escape and induce a potent antitumor response. In preclinical models of cancer, single-agent therapy with IDO inhibitors showed modest antitumor activities.[8,9] There have been some reports on the combination of IDO inhibitors and common chemotherapeutics in murine tumor models.[8,12,17] Combination of IDO inhibitors with chemotherapy may be a potential way to improve therapeutic benefits in the clinic. It is essential to investigate the dose and schedule of the combinatorial treatment in preclinical studies, which will be beneficial for effective translation of this approach to the clinic.

IDO might be involved in the regulation of tumor resistance to PTX.[15] Therefore, the effects of NLG919 on the sensitivity of B16-F10 cells to PTX were preliminarily studied. NLG919 significantly increased the cytotoxic activity of PTX toward B16-F10 cells after the cells were pretreated with IFN-γ, while there was no such effect in the absence of IFN-γ induction. The mechanistic basis for this increase is not yet clear, and further studies are needed. The possible mechanism may be that IDO is induced by IFN-γ, which further activates the apoptosis-related signaling pathways, resulting in enhanced cytotoxic activity.

In the B16-F10-bearing mouse model, NLG919 suppressed B16-F10 tumor growth and Kyn levels in a dose-dependent manner and achieved the maximum efficacy at 100 mg/kg. The data also indicated that the level of Kyn was suitable as a biomarker for evaluating the therapeutic activity of NLG919. In the study of the combinatorial treatment, three different regimens of PTX were used, which represented different doses at the same dosing frequency, as well as different frequencies at the same dose. NLG919 combined with the different regimens of PTX displayed synergistic antitumor effects by increasing the percentage of $CD3^+$, $CD8^+$, and $CD4^+$ T cells, enhancing the secretion of IFN-γ and IL-2, and decreasing the percentage of $CD4^+CD25^+$ Tregs. No significant effect of NLG919 on the body weight of the tumor-bearing mice was observed in any of the animal studies, and NLG919 did not increase the toxic effects of PTX, indicating that the combination treatment with NLG919 and PTX was well tolerated. However, one limitation of this study was that only the B16-F10 cell line was used, and further studies in other tumor models will be performed later to confirm the reproducibility of the data.

In summary, our findings indicate that NLG919 can potentiate the antitumor efficacy of PTX without increasing its side effects and suggest the combination of IDO inhibitor-based immunotherapy with chemotherapy as a new potential strategy for cancer treatment.

Acknowledgements

The first two authors (Xiangjing Meng and Guangying Du) contributed equally to this work and should be considered co-first authors.

Declaration of conflicting interests

The author(s) declared no potential conflicts of interest with respect to the research, authorship, and/or publication of this article.

Funding

This work was supported by the National Natural Science Foundation of China (grant no. 81473188), Shandong Provincial Natural Science Foundation (Young and Middle-Aged Scientists Research Awards Fund; grant no. BS2015YY012), Project of Shandong Province Higher Educational Science and Technology Program (grant no. J15LM03), Doctoral Fund of Yantai University (grant no. YX13B29), and Taishan Scholar Project awarded to Zimei Wu. The funders had no role in study design, data collection and analysis, decision to publish, or preparation of the manuscript.

References

1. Sharma P and Allison JP. The future of immune checkpoint therapy. *Science* 2015; 348: 56–61.
2. Markham A. Atezolizumab: First global approval. *Drugs* 2016; 76: 1227–1232.
3. Ferdinande L, Demetter P, Perez-Novo C, et al. Inflamed intestinal mucosa features a specific epithelial expression pattern of indoleamine 2,3-dioxygenase. *International Journal of Immunopathology and Pharmacology* 2008; 21: 289–295.
4. Iacobucci I, Di Rora AG, Falzacappa MV, et al. In vitro and in vivo single-agent efficacy of checkpoint kinase inhibition in acute lymphoblastic leukemia. *Journal of Hematology & Oncology* 2015; 8: 125.
5. Prendergast GC, Smith C, Thomas S, et al. Indoleamine 2,3-dioxygenase pathways of pathogenic inflammation and immune escape in cancer. *Cancer Immunology, Immunotherapy* 2014; 63: 721–735.
6. Selvan SR, Dowling JP, Kelly WK, et al. Indoleamine 2,3-dioxygenase (IDO): Biology and target in cancer immunotherapies. *Current Cancer Drug Targets* 2016; 16: 755–764.
7. Moon YW, Hajjar J, Hwu P, et al. Targeting the indoleamine 2,3-dioxygenase pathway in cancer. *Journal for Immunotherapy of Cancer* 2015; 3: 51.
8. Muller AJ, DuHadaway JB, Donover PS, et al. Inhibition of indoleamine 2,3-dioxygenase, an immunoregulatory target of the cancer suppression gene Bin1, potentiates cancer chemotherapy. *Nature Medicine* 2005; 11: 312–319.
9. Uyttenhove C, Pilotte L, Theate I, et al. Evidence for a tumoral immune resistance mechanism based on tryptophan degradation by indoleamine 2,3-dioxygenase. *Nature Medicine* 2003; 9: 1269–1274.
10. Dalgleish AG. Rationale for combining immunotherapy with chemotherapy. *Immunotherapy* 2015; 7: 309–316.
11. Cook AM, Lesterhuis WJ, Nowak AK, et al. Chemotherapy and immunotherapy: Mapping the road ahead. *Current Opinion in Immunology* 2016; 39: 23–29.
12. Li M, Bolduc AR, Hoda MN, et al. The indoleamine 2,3-dioxygenase pathway controls complement-dependent enhancement of chemo-radiation therapy against murine glioblastoma. *Journal for Immunotherapy of Cancer* 2014; 2: 21.
13. Javeed A, Ashraf M, Riaz A, et al. Paclitaxel and immune system. *European Journal of Pharmaceutical Sciences* 2009; 38: 283–290.
14. Mario R, Mautino, Firoz A, et al. NLG919, a novel indoleamine-2,3-dioxygenase (IDO)-pathway inhibitor drug candidate for cancer therapy. In: *Proceedings of AACR 104th annual meeting*, Washington, DC, 6–10 April 2013, Abstract number 491.
15. Takikawa O. Biochemical and medical aspects of the indoleamine 2,3-dioxygenase-initiated L-tryptophan metabolism. *Biochemical and Biophysical Research Communications* 2005; 338: 12–19.
16. Kilinc MO, Aulakh KS, Nair RE, et al. Reversing tumor immune suppression with intratumoral IL-12: Activation of tumor-associated T effector/memory cells, induction of T suppressor apoptosis, and infiltration of CD8+ T effectors. *Journal of Immunology* 2006; 177: 6962–6973.
17. Salvadori ML, da Cunha Bianchi PK, Gebrim LH, et al. Effect of the association of 1-methyl-DL-tryptophan with paclitaxel on the expression of indoleamine 2,3-dioxygenase in cultured cancer cells from patients with breast cancer. *Medical Oncology* 2015; 32: 248.